HIGH ENERGY γ-RAYS: A PROBE FOR MOMENTUM- AND ENERGY-DISTRIBUTIONS IN THE REACTION ZONE? ☆

W. CASSING, T. BIRO [1], U. MOSEL, M. TOHYAMA

Institut für Theoretische Physik, Universität Giessen, D-6300 Giessen, Fed. Rep. Germany

and

W. BAUER [2]

Cyclotron Laboratory, Michigan State University, East Lansing, MI 48824, USA

Received 18 July 1986; revised manuscript received 8 September 1986

Double-differential cross sections are calculated for high-energy γ-ray emission in intermediate-energy nucleus–nucleus collisions on the basis of individual nucleon–nucleon bremsstrahlung. Using a microscopic phase-space model for first-chance nucleon–nucleon collisions and a semiclassical expression for p–n bremsstrahlung agreement is found with experimental data from roughly 40 MeV/u to 84 MeV/u.

Recent experiments on energetic photon emission in intermediate-energy nucleus–nucleus collisions show a large yield of energetic γ-rays with energies above 50 MeV [1–6]. The origin of these photons which may carry a considerable amount of the total energy available in the CM system is still not understood. Do we see collective bremsstrahlung as suggested in refs. [7–9], thermal emission from hot spots [10], nucleon–nucleon bremsstrahlung [4,5, 10] or just statistical effects in an equilibrated A-body phase space [11]?

Meanwhile, there are indications against collective bremsstrahlung both from theoretical studies [12,13] as well as from experimental data [2,4,5], since experimental angular distributions of energetic photons turn out to be rather isotropic in the nucleon–nucleon center-of-mass system (see, however, ref. [6]). On the other hand, experiments looking for energetic proton or neutron emission [14] are inconsistent with the assumption of complete equilibration in phase space indicating that energetic γ-rays might carry information about the nonequilibrium phase of nucleus–nucleus collisions. Indeed, energetic photons are quite promising in this respect since their scattering and reabsorption, contrary to nucleons and pions, is very small. In the case when energetic γ-rays are produced in the very early stage of the collision, what is the mechanism?

In this letter we explore the possibility that the observed high-energy γ-rays come primarily from incoherent collisions of energetic nucleons. Both the ppγ as well as the pnγ reactions have been studied experimentally [15]. Due to a destructive interference of the photons emitted from the two proton lines the ppγ cross section is smaller than that for pnγ by more than an order of magnitude. We, therefore, include only the latter process in our model. The incoherent summation over the many possible np collisions in the Fermi-sea is then performed in an extended version of the first-collision model [16]. We note that the first-collision model is known to describe the high-energy photon emission from proton–nucleus collisions [13,17].

☆ Supported by BMFT and GSI Darmstadt.
[1] On leave from CICP, H-1525 Budapest, Hungary.
[2] Supported by Studienstiftung des Deutschen Volkes.

A proton impinging on a nucleus in its ground-state only moderately changes the selfconsistent mean field in which the nucleons of the target are bound. Neglecting correlations between nucleons it is thus justified to represent the state of the target nucleons by a ground-state Slater determinant or equivalently by a ground-state phase-space distribution. In the case of nucleus–nucleus collisions, however, the projectile and target nucleus are in the interaction zone far from being in their respective ground-state Slater-determinants since even on the one-body level the selfconsistent mean field is a rapidly changing function of time. The appropriate quantal phase-space distribution is given now by the Wigner function:

$$f(r,k;\omega,t)=\sum_{\alpha\ \mathrm{occ}}\int \mathrm{d}^3s\ \mathrm{d}\tau \exp(-\mathrm{i}k\cdot s+\mathrm{i}\omega\tau)$$

$$\times\ \varphi_\alpha(r+\tfrac{1}{2}s,\ t+\tfrac{1}{2}\tau)\varphi_\alpha^*(r-\tfrac{1}{2}s,t-\tfrac{1}{2}\tau)\,. \qquad (1)$$

where the $\varphi_\alpha(r,t)$ denote time-dependent s.p. states as evaluated e.g. selfconsistently from TDHF [18] for fixed spin σ and isospin τ. The quantity $f(r,k;\omega,t)$ has been studied extensively in the case of intermediate-energy heavy-ion collisions in refs. [19,20]. There it has been found that the microscopic momentum distributions differ significantly from that given by two shifted Fermi-spheres; this difference has a large influence on the cross section for pion production [19–21].

The average phase-space distribution in the reaction zone is given by

$$f_{\mathrm{av}}(k;t)=\frac{1}{2\pi V_0}\int \mathrm{d}\omega \int_{V_0} \mathrm{d}^3r\, f(r,k;\omega,t)\,, \qquad (2)$$

where V_0 is a finite volume around r_0 while r_0 denotes the spacial center of the reaction zone. Using a value of $V_0 \geqslant 50\ \mathrm{fm}^3$, the rapid oscillations present in the quantum mechanical f, which reflect the uncertainty principle, disappear in f_{av}. The averaged distribution (2) is shown in fig. 1 for various times in units of fm/c for a head-on collision of $^{40}\mathrm{Ca}+{}^{40}\mathrm{Ca}$ at 80 MeV/u as a function of $k_\perp := (k_x = 0, k_y)$ and $k_\parallel = k_z$ in obvious notation. We find a considerable open phase space for $k_\parallel \approx 0$ and in addition high-momentum components for $|k| > 2.5\ \mathrm{fm}^{-1}$, which do not appear in the infinite nuclear matter limit.

Next we define an average initial momentum distribution $g(k)$ in the reaction zone by

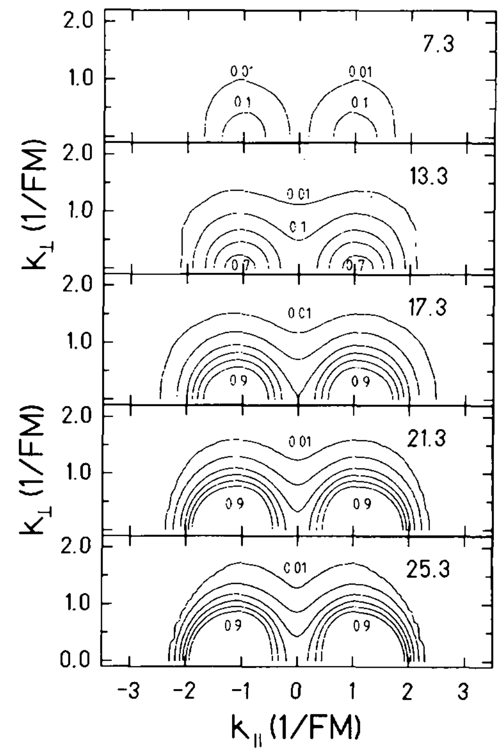

Fig. 1. The average microscopic momentum distribution in the reaction zone (2) for a central collision of $^{40}\mathrm{Ca}+{}^{40}\mathrm{Ca}$ at 80 MeV/u as a function of $k_\parallel$ and $k_\perp$. The contour lines correspond to cuts of 10^{-2}, 0.1, 0.3, 0.5, 0.7, and 0.9 in obvious sequence while the time is given in units of fm/c.

$$g(k)=\Delta t^{-1}\int_{t_0}^{t_0+\Delta t} \mathrm{d}t\, f_{\mathrm{av}}(k;t)\,, \qquad (3)$$

where t_0 denotes the time at which the relative distance R_{rel} is given by the touching configuration of the nuclear densities which may be defined by

$$R_{\mathrm{rel}}(t_0)=1.4\,(A_1^{1/3}+A_2^{1/3})\ [\mathrm{fm}]\,. \qquad (4)$$

The time interval Δt is fixed to be equal to the average collision time τ of energetic nucleons in the reaction zone which is about 7–10 fm/c [21]. We use $\Delta t = 10$ fm/c and note that by changing Δt in eq. (3) by 50% our final results are only modified by about 10%; this uncertainty is well below the uncertainty of the data. We thus assume that $g(k)$ in eq. (3) properly describes the average phase-space distribution in the reaction zone prior to equilibration by two-body collisions.

The basic assumption of the first collision model is that high-energy particles (in this case photons) are emitted before the initial momentum distributions is degraded due to nuclear interactions. By using $g(\boldsymbol{k})$ from eq. (3), which is obtained from a TDHF calculation via (1) and (2) and thus contains interaction effects in the mean-field approximation, we go beyond the simplest model in which the momentum distributions of the free, noninteracting nuclei are used. Our main assumption then is that the high-momentum components and the "Fermi-hole" at $k_{\parallel} = 0$ do not decay due to two-body collisions before the photons are emitted. This decay time is calculated to be about 7–10 fm/c at the bombarding energies considered here [19–21].

The effective double-differential cross section for γ-production in single nucleon–nucleon collisions in the nuclear medium is then given by

$$\frac{\mathrm{d}^2\sigma^{\mathrm{eff}}}{\mathrm{d}\omega\,\mathrm{d}\Omega_\gamma} = \int \mathrm{d}^3k_1\,\mathrm{d}^3k_2\,g^+(\boldsymbol{k}_1)g^-(\boldsymbol{k}_2)$$

$$\times \int \frac{\mathrm{d}\Omega_q}{4\pi}\,\frac{\omega}{\omega'}\,\frac{\mathrm{d}^2\sigma^0}{\mathrm{d}\omega'\mathrm{d}\Omega'_\gamma}\,P(\boldsymbol{k}'_1,\boldsymbol{k}'_2)N_c^{-1}\,. \tag{5}$$

Here the $g^{\pm}(\boldsymbol{k})$ are the momentum distributions in the individual nuclei:

$$g^{\pm}(\boldsymbol{k}) = g(\boldsymbol{k})\theta(\pm k_{\parallel})\,. \tag{6}$$

The cross section $\mathrm{d}^2\sigma^0/\mathrm{d}\omega_\gamma\mathrm{d}\Omega_\gamma$ describes the production of a photon with energy ω_γ in a collision of nucleons with initial momenta $\boldsymbol{k}_1$ and $\boldsymbol{k}_2$ into the direction $\mathrm{d}\Omega'_\gamma$ in the individual NN CM frame. N_c gives, up to a factor, the total number of collisions in the reaction zone:

$$N_c = \int \mathrm{d}^3k_1 g^+(\boldsymbol{k}_1) \int \mathrm{d}^3k_2 g^-(\boldsymbol{k}_2)\,, \tag{7}$$

so that the integrations over $\boldsymbol{k}_1$ and $\boldsymbol{k}_2$ in eq. (5) achieve an averaging over all possible initial momenta. The factor $P(\boldsymbol{k}'_1,\boldsymbol{k}'_2)$ gives the probability that the final state with particle momenta $\boldsymbol{k}'_1$ and $\boldsymbol{k}'_2$ is Pauli-allowed:

$$P(\boldsymbol{k}'_1,\boldsymbol{k}'_2) = [1 - g(\boldsymbol{k}'_1)]\,[1 - g(\boldsymbol{k}'_2)]\,. \tag{8}$$

The final momenta are determined by energy $\delta(\hbar^2/2M(k_1^2 + k_2^2 - k_1'^2 - k_2'^2) - \omega)$ and momentum conservation $\delta_3(\boldsymbol{k}_1 + \boldsymbol{k}_2 - \boldsymbol{k}'_1 - \boldsymbol{k}'_2 - \boldsymbol{k}'_\gamma)$. These four constraints leave only the direction of the particle relative momentum

$$\boldsymbol{q} = \tfrac{1}{2}(\boldsymbol{k}'_1 - \boldsymbol{k}'_2) \tag{9}$$

free; its solid angle is denoted by $\mathrm{d}\Omega_q$ in (5). By incorporating the energy conservation in (5) we use an essential result from the studies in refs. [19–21], namely that due to the rapid time-dependence of the mean field in the collision zone the nucleons can be considered to be on-shell so that the free-particle energy–momentum relation

$$\omega(k) = \hbar^2k^2/2M \tag{10}$$

can be employed there. More precisely: the microscopic Wigner function (1) averaged over space and time as in eqs. (2) and (3) may well be approximated by

$$\bar{f}(\boldsymbol{k},\omega) = g(\boldsymbol{k})\delta(\omega - \hbar^2k^2/2M) \tag{11}$$

for heavy-ion collisions with energies $\geqslant$40 MeV/u. For low bombarding energies and/or nuclei close to the ground-state more complicated energy–momenrum relations have to be used [20]. Furthermore, the δ-function in energy implies that we consider all transitions to be on-shell. Indeed, a collision frequency of $\tau = 10$ fm/c allows for an uncertainty in energy of about 20 MeV. However, we do not want to speculate about off-shell phenomena. We just intend to compare our expectation for energetic photon yields from first-change pn → pnγ on-shell reactions in nucleus–nucleus collisions with experimental data. Large discrepancies then could indicate the necessity of off-shell transitions (see, however, below).

The elementary NNγ cross section could in principle be evaluated by attaching outgoing γ-lines to the external legs of a T-matrix for NN scattering and including the exchange-current contributions [22]. Since this is quite an involved program and we are not primarily interested in a detailed description of the elementary process, we employ here a semiclassical expression describing the emission of photons in a hard-sphere scattering process [23]

$$\mathrm{d}^2\sigma^0/\mathrm{d}\omega\,\mathrm{d}\Omega = (R^2e^2/12\pi c^3\omega\hbar)$$

$$\times\,(3v_\mathrm{i}^2\sin^2\theta + 2v_\mathrm{f}^2)\theta(Mv_\mathrm{i}^2 - \omega)\,, \tag{12}$$

with $v_\mathrm{f}^2 = v_\mathrm{i}^2 - \omega/M$.

Here the expression given in ref. [23] has been generalized by explicitly introducing the initial and final velocity v_i and v_f, respectively, in the NN CM system. In this way energy conservation is restored in the elementary process while momentum conservation follows from (5). The toal energy- and angle-integrated cross section for photons with energies above 40 MeV as measured in pnγ at 140 MeV and 200 MeV [15,24] is reproduced by (12) if the hard-sphere scattering radius is chosen to be $R \approx 2.1$ fm. Although eq. (12) gives a poor description of the elementary NNγ process as far as the spectrum and the angular distributions are concerned, it is nevertheless still quite adequate for our purpose since (12) is integrated over wide distributions in (5) so that the details of (12) are washed out in the effective cross section (5). We note that using alternative expressions for (12), as e.g. employed by Nifenecker and Bondorf [10], the final results are only modified on the 10% level.

The total yield of γ-rays in a nucleus–nucleus collision furthermore is given by the number of first-chance proton–neutron collision for given impact parameter b and final integration over b. Geometrical considerations as e.g. described in ref. [25] and standard values for the nuclear radius as well as the average nucleon–nucleon cross section at energies larger than 50 MeV yield the final expression

$$\begin{aligned} \mathrm{d}^2\sigma/\mathrm{d}\omega\,\mathrm{d}\Omega_\gamma|_{A_1+A_2} &= [(\mathrm{d}^2\sigma^{\mathrm{eff}}/\mathrm{d}\omega\,\mathrm{d}\Omega_\gamma)/\sigma_{\mathrm{np}}] \\ &\times (\pi R_1^2 \pi R_2^2/\sigma_{\mathrm{np}})[(N_1Z_2+N_2Z_1)/A_1A_2] \\ &\approx 2.3 \times (N_1Z_2+N_2Z_1)/(A_1A_2)^{1/3} \\ &\times \mathrm{d}\sigma^{\mathrm{eff}}/\mathrm{d}\omega\,\mathrm{d}\Omega_\gamma, \end{aligned} \tag{13}$$

where N_i, Z_i, A_i denote neutron number, proton number and mass number of projectile and target; the total np cross section σ_{np} is 30 mb according to ref. [26].

The evaluation of $\mathrm{d}^2\sigma/\mathrm{d}\omega\,\mathrm{d}\Omega_\gamma$ along the line of eqs. (5)–(13) is straightforward and does not involve free parameters. Results for the double differential photon yield at $\theta_\gamma = 90°$ in the NN CM system are shown in fig. 2 for $^{12}C + {}^{12}C$ at laboratory energies from 40 MeV/u to 140 MeV/u. The spectra are roughly exponential in energy and almost isotropic in angle. When fitting exponentials to the spectra for 50 MeV $< \omega_\gamma <$ 100 MeV, a linear increase of the slope parameter E_0 with the bombarding energy per nucleon is found. This is displayed in fig. 3 by the two dashed lines which represent the upper and lower limit for slope parameters from the calculated spectra. Corresponding experimental slope parameters from refs. [1–3] are indicated by ⧫ showing no significant discrepancy.

Since experimental yields are roughly isotropic in

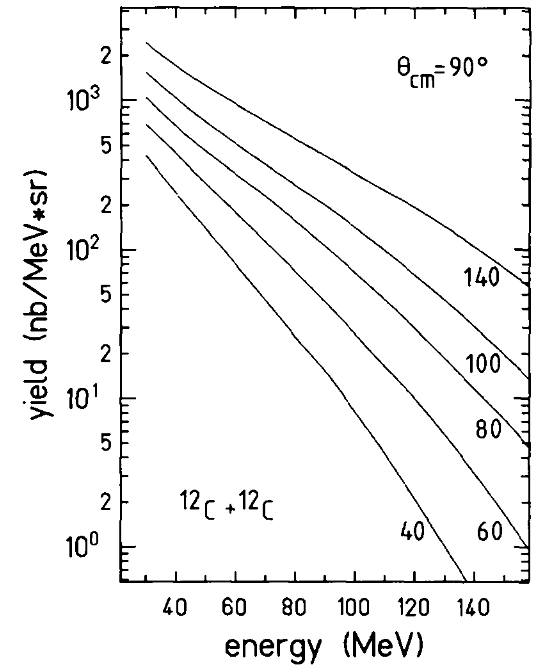

Fig. 2. Double-differential photon spectra at $\theta_\gamma = 90°$ in the nucleon–nucleon CMS for $^{12}C + {}^{12}C$ at various bombarding energies in MeV/u.

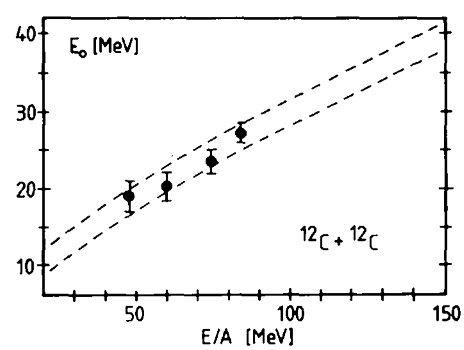

Fig. 3. Comparison of slope parameters E_0 extracted from fig. 2 for 50 MeV $\leqslant \omega_\gamma \leqslant$ 100 MeV (upper and lower dashed line) with corresponding experimental values ⧫ from refs. [1,3].

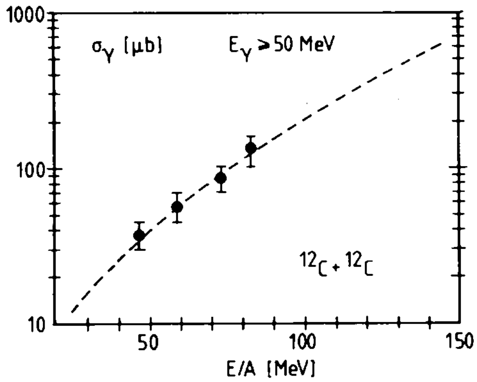

Fig. 4. Inclusive cross section for high-energy photons above 50 MeV according to first-change proton–neutron bremsstrahlung (dashed line) in comparison with experimental results from ref. [1] for $^{12}C + ^{12}C$ at various laboratory energies per nucleon.

the nucleon–nucleon center-of-mass frame and exponential in energy, too, it is sufficient to compare the total yields. This comparison is shown in fig. 4 for $^{12}C + ^{12}C$ as a function of the lab bombarding energy per nucleon for energetic photons above 50 MeV. Experimental data have been adopted from ref. [1]. We find that our results are well within the experimental error bars, which indicates that not substantially more than primary proton–neutron collisions are needed to understand the present data on energetic photon production. Essential for this conclusion is the use of the microscopic phase-space distribution (3). We note again that our results are quite insensitive to the use of alternative expressions for the elementary pnγ cross section (12) as long as the total pnγ yield is reproduced correctly.

In summary, we have calculated double-differential cross sections for high-energy photon emission in intermediate-energy nucleus–nucleus collisions on the basis of a first-collision model in which the total γ-yield is made up from the incoherent superposition of individual on-shell pnγ processes. The momentum distributions, which are an essential ingredient for this model, have been obtained from a time-dependent description of the collision dynamics. Based on our earlier results [12] we conclude that while at most 10% of the observed cross section is due to collective nucleus–nucleus bremsstrahlung, the dominant part of the total yield is due to first-chance pn collisions; this conclusion agrees with the results obtained by Nakayama and Bertsch [13]. We thus propose that high-energy photons carry information about the energy- and momentum-distributions of nucleons in the reaction zone during the very early stages of the collision. Note, however, that present data appear to be also compatible with the picture of pn-bremsstrahlung in a nuclear fireball [27].

The authors like to thank E. Grosse, H. Noll, H. Heckwolf, N. Herrmann, A. Gobbi, P. Braun-Munzinger, W. Benenson and F. Plasil for stimulating discussions. We are particularly indebted to G.F. Bertsch for many helpful remarks and a critical reading of the manuscript. Furthermore, we acknowledge the use of the 3D-TDHF computer code by R. Cusson.

References

[1] E. Grosse et al., preprint GSI-86-9, submitted to Europhys. Lett.
[2] N. Herrmann et al., GSI Annual Report (1985).
[3] H. Heckwolf, GSI-Report 86-3.
[4] J. Stevenson et al., Contrib. Workshop on Nuclear dynamics (Copper Mountain, February 1986), and to be published.
[5] H. Nifenecker et al., Proc. XIV Intern. Winter Meeting on Nuclear physics (Bormio, January 1986).
[6] N. Alamanos et al., submitted to Phys. Lett. B.
[7] E.M. Nyman, Phys. Lett. B 136 (1984) 143.
[8] D. Vasak et al., Nucl. Phys. A 428 (1984) 291c.
[9] C.M. Ko et al., Phys. Rev. C 31 (1985) 2324.
[10] H. Nifenecker and J.P. Bondorf, Nucl. Phys. A 442 (1985) 478.
[11] R. Shyam and J. Knoll, Nucl. Phys. A 448 (1986) 322.
[12] W. Bauer et al., Nucl. Phys. A 456 (1986) 159.
[13] K. Nakayama and G.F. Bertsch, to be published.
[14] E. Holob et al., Phys. Rev. C 28 (1983) 252; C.K. Gelbke, Nucl. Phys. A 400 (1983) 473c.
[15] P.F.M. Koehler et al., Phys. Rev. Lett. 18 (1967) 933.
[16] G.F. Bertsch, Phys. Rev. C 15 (1977) 713.
[17] J.A. Edgington and B. Rose, Nucl. Phys. A 89 (1966) 523.
[18] R.Y. Cusson et al., Phys. Rev. Lett. 36 (1976) 1166; Phys. Rev. C 18 (1978) 2589; Phys. Rev. Lett. 42 (1979) 694.
[19] W. Cassing, Phase-space approach to nuclear dynamics, ed. M. Di Toro (World Scientific, Singapore, 1986) pp. 64–93.
[20] W. Cassing, preprint University of Giessen, submitted to Z. Phys. A.
[21] W. Cassing, Habilitationsschrift TH Darmstadt (1985) GSI Report 86-6.

[22] R. Baier et al., Nucl. Phys. B 11 (1969) 675;
G.E. Bohannon et al., Phys. Rev. C 16 (1977) 16;
V.R. Brown and J. Franklin, Phys. Rev. C 8 (1973) 1706.
[23] J.D. Jackson, Classical electrodynamics (Wiley, New York, 1962) p. 733.
[24] F.P. Brady et al., Phys. Rev. Lett. 20 (1968) 750.
[25] J. Knoll and J. Randrup, Nucl. Phys. A 324 (1979) 445; Phys. Rev. Lett. B 103 (1981) 264;
J. Cugnon, J. Knoll and J. Randrup, Nucl. Phys. A 360 (1981) 444.
[26] K. Chen et al., Phys. Rev. 166 (1968) 949.
[27] D. Neuhauser and S.E. Koonin, preprint MAP-80, submitted to Nucl. Phys. A.